Adaptive IMRT using a multiobjective evolutionary algorithm integrated with a diffusion–invasion model of glioblastoma

2012 Phys. Med. Biol. 57 8271

(http://iopscience.iop.org/0031-9155/57/24/8271)

IOP Publishing Physics in Medicine and Biology

Phys. Med. Biol. **57** (2012) 8271–8283 doi:10.1088/0031-9155/57/24/8271

Adaptive IMRT using a multiobjective evolutionary algorithm integrated with a diffusion–invasion model of glioblastoma

C H Holdsworth[1,2], D Corwin[3], R D Stewart[1], R Rockne[3], A D Trister[1,4], K R Swanson[3] and M Phillips[1]

[1] Department of Radiation Oncology, University of Washington Medical Center, 1959 N E Pacific Street, Seattle, WA 98195, USA
[2] Department of Radiation Oncology, Brigham and Women's Hospital, 75 Francis Street, Boston, MA 02115, USA
[3] Department of Neurological Surgery, Northwestern University, 676 N St Clair St, Chicago, IL 60611, USA
[4] Department of Systems Biology, Sage Bionetworks, 1100 Fairview Avenue N, Seattle, WA 98109, USA

E-mail: choldsworth@partners.org

Received 16 August 2012, in final form 10 October 2012
Published 29 November 2012
Online at stacks.iop.org/PMB/57/8271

Abstract

We demonstrate a patient-specific method of adaptive IMRT treatment for glioblastoma using a multiobjective evolutionary algorithm (MOEA). The MOEA generates spatially optimized dose distributions using an iterative dialogue between the MOEA and a mathematical model of tumor cell proliferation, diffusion and response. Dose distributions optimized on a weekly basis using biological metrics have the potential to substantially improve and individualize treatment outcomes. Optimized dose distributions were generated using three different decision criteria for the tumor and compared with plans utilizing standard dose of 1.8 Gy/fraction to the CTV (T2-visible MRI region plus a 2.5 cm margin). The sets of optimal dose distributions generated using the MOEA approach the Pareto Front (the set of IMRT plans that delineate optimal tradeoffs amongst the clinical goals of tumor control and normal tissue sparing). MOEA optimized doses demonstrated superior performance as judged by three biological metrics according to simulated results. The predicted number of reproductively viable cells 12 weeks after treatment was found to be the best target objective for use in the MOEA.

(Some figures may appear in colour only in the online journal)

1. Introduction

Glioblastoma multiforme (GBM) is the most common primary brain malignancy and is characterized by extensive infiltration of normal tissue. This highly resilient tumor cannot be cured using current clinical methods, and patients have a median survival of approximately

14 months with the standard of care including surgery, radiation and chemotherapy (Stupp *et al* 2005). These therapies are often limited by the potential toxicities to the normal brain.

Large clinical target margins and volumes are routinely used in radiation therapy of GBM due to its widely diffuse nature. Based on a number of dose escalation trials for GBM, a dose of ∼50 Gy in standard fractions to the clinical target volume (CTV) of the T2 enhancing region plus a 2.5 cm margin followed by a boost dose of ∼10 Gy to the gross tumor volume of the T1Gd enhancing region plus a 2 cm margin results in a modest prolongation in patient survival with low risk of radiation necrosis and cognitive decline within the first 12–24 months after treatment (Lawrence *et al* 2010). However, uniform prescription doses such as these do not take into account the patient-specific diffuse disease distribution peripheral to the imaging abnormality or the biological tumor heterogeneity of these tumors. Other tissue-level factors governing the response, reoccurrence and progression of disease such as hypoxia (Brown 2000, Carlson *et al* 2011), genomic instability (Perez-Garcia *et al* 2012), and the presence of cancer stem cells (Binda *et al* 2012) are also not considered in these non-optimized plans.

As an alternative to the standard practice of prescribing uniform doses to targets, IMRT can be used to deliver non-uniform dose distributions that are tailored to patient-specific, biological, and spatial metrics derived from models of tumor and normal cell radiation response. An optimal treatment plan must incorporate the effects of radiation with respect to both cancer cells and normal tissue in addition to the evolving cell distributions during a course of treatment (Tome and Fowler 2003). The high level of spatial complexity required to optimize these treatment plans is challenging using conformal dose delivery methods, but may be quite practical by combining IMRT with biologically based plan optimization.

In multiobjective IMRT optimization, a plan is only considered to *dominate* (be superior to) another plan if all of its decision criteria (clinical objectives) are more optimal than all of the decision criteria of the inferior plan. Each structure (target or OAR) typically has one decision criteria, so one IMRT plan with more uniform target coverage may have higher dose to OARs than another IMRT plan with worse target coverage. In this case, neither plan would dominate or be considered superior to the other in a multiobjective context. Hence, in multiobjective IMRT optimization there is no single optimal plan, and the best possible solution is the set of plans that cannot be dominated and that represents the optimal tradeoffs amongst all decision criteria. This set is known as the Pareto Front.

Current practice in radiation therapy is to assume a steady state model of the tumor and to optimize based on the size and location of the tumor at the beginning of treatment. Tumor growth is occasionally accounted for in different fractionation schedules by calculating the biologically equivalent dose with a term included for repopulation. In this work, strategies for biologically-guided radiation therapy (Stewart and Li 2007) are used to examine potential gains in treatment effectiveness that are possible by combining a patient-specific, diffusion–invasion model of glioblastoma (Rockne *et al* 2009a, Rockne *et al* 2010) with a multiobjective evolutionary algorithm (MOEA) for dose optimization (Holdsworth *et al* 2010, Holdsworth *et al* 2011, Holdsworth *et al* 2012). We present an algorithm for IMRT optimization that includes the effects of radiation-induced cell kill, tumor diffusion and proliferation. The optimization algorithm accounts for the temporal development of the tumor by performing weekly optimizations and by including the future state of the tumor in the optimization objectives.

2. Methods

2.1. Linear-quadratic (LQ) cell survival model and equivalent uniform dose (EUD)

In the LQ model (Hall 1994), the fraction of cells, S, that survive absorbed dose d (Gy), delivered to a region of tissue in n fractions, is given as $S(nd) = \exp(-\alpha nd - \beta G n^2 d^2)$, where

α (Gy^{-1}) and β (Gy^{-2}) are intra- and inter-track radiation sensitivity parameters and G is the Lea–Catcheside dose-protraction factor (Sachs *et al* 1997). For a typical radiation therapy treatment consisting of n well separated fractions, G can be approximated by $G \cong 1/n$ (Stewart and Li 2007), and the LQ survival model can be re-written as $\mathrm{S}(nd) = \exp(-\alpha nd - \beta nd^2)$. In this study, we used $\alpha = 0.12\ \mathrm{Gy}^{-1}$ and $\alpha/\beta = 3$ Gy for normal brain tissue.

Equivalent uniform dose (EUD) is a method for quantifying non-uniform dose distributions. EUD is defined as the absorbed dose, which if uniformly delivered to a tissue region of interest, will produce the same biological effect as delivery of the non-uniform dose distribution to the same tissue region of interest (Niemierko 1997). To compute this we solve iteratively for EUD as shown in equation (1):

$$\sum_i c_i v_i \, \mathrm{e}^{-\alpha d_i - \beta_i d_i^2} = \left[\sum_i c_i v_i \right] \mathrm{e}^{-\alpha \mathrm{EUD} - \beta \mathrm{EUD}^2}, \tag{1}$$

where c_i, v_i and d_i represent the cell density, volume and dose, respectively, at the spatial location indicated by i.

2.2. Mathematical model of GBM

A patient-specific, proliferation-invasion (PI-RT) mathematical model of GBM (Rockne *et al* 2009, Rockne *et al* 2010) describes the change in tumor cell density with respect to time and space by quantifying net rates of proliferation (ρ time^{-1}) and invasion (D area/time). The radiosensitivity parameters α and β in the PI-RT model are the same as in LQ cell survival model. Patient-specific PI-RT parameters, except normal tissue radiosensitivity parameters, were determined from routinely available pre-treatment MRI imaging (Swanson *et al* 2003, 2008a, Harpold *et al* 2007, Wang *et al* 2009b, Szeto *et al* 2009, Rockne *et al* 2010). Tumor-specific estimates of α have been shown to correlate linearly with the proliferation parameter ρ and can be determined for any patient *a priori* to radiation treatment, assuming the ratio α/β is assumed to be fixed at 10 Gy (Rockne *et al* 2010).

Tumor cell density evolves in both space and time and represents net density per unit volume, not the behavior of individual cells. Proliferation is assumed to follow a logistic growth curve while invasion is modeled as a Fickian diffusion process. The model is of the form:

$$\frac{\partial c}{\partial t} = \nabla \cdot (D \nabla c) + \rho c \left(1 - \frac{c}{k}\right) - Rc \left(1 - \frac{c}{k}\right), \tag{2}$$

where ρ is the rate of proliferation, D is the rate of diffusion, k is the maximum allowed tumor cell concentration, c is the tumor cell distribution as a function of space and time:

$$c = c(\mathbf{x}, t) \tag{3}$$

and

$$R = \begin{cases} 0, & \text{between daily fractions} \\ 1 - S(\alpha, \beta, d(\mathbf{x}, t)), & \text{otherwise} \end{cases} \tag{4}$$

where $d(\mathbf{x}, t)$ is the radiation dose distribution and S is the estimated surviving fraction using the LQ cell survival model with the parameters α and β.

The GBM model uses a 'tip of the iceberg' view of clinical imaging, where the boundaries of the enhancing regions on T1Gd and T2 MRIs are associated with isosurfaces of constant density. These isosurfaces are used to infer a gradient of tumor cells, characterized by an invisibility index, the ratio of model parameters D/ρ (Rockne *et al* 2010, Szeto *et al* 2009, Wang *et al* 2009b, Harpold *et al* 2007). The GBM model is a form of the well-studied Fisher's equation, with solutions that approach a traveling wave with a constant velocity of $2\sqrt{D\ \rho}$

Table 1. GBM model parameters used for study patients.

Patient	T1Gd radius at diagnosis (cm)	T2 radius at diagnosis (cm)	T1Gd radius at second timepoint (cm)	T2 radius at second timepoint (cm)	Time between scans (days)	D (cm^2 yr^{-1})	ρ (/yr)	α (/Gy)
1	1.7	2.2	1.7	2.0	13	0.11	13.68	0.02
2	1.3	1.6	1.5	1.9	19	0.09	50.29	0.27

(Fisher 1937). This is in agreement with observed linear velocities on serial MRI of untreated low-grade gliomas followed over as many as 15 years (Mandonnet *et al* 2003) as well as untreated GBM (Swanson *et al* 2002). With these two equations, we can solve for the patient-specific model parameters D and ρ algebraically as in (Rockne *et al* 2010, Szeto *et al* 2009, Wang *et al* 2009b, Harpold *et al* 2007).

Results presented in the work are based on data obtained from two patients. The GBM model parameters used for patients were derived from MRI images taken before and after standard radiation therapy. The values used for patient 1 with relatively radio-resistant glioblastoma and for patient 2 with relatively radio-sensitive disease are given in table 1 (patients 6 and 5 in Rockne *et al* 2010, respectively). Results were calculated for the standard of care plan that was generated for clinical use that delivered 61.2 Gy in 1.8 Gy daily fractions to the CTV over 7 weeks. In order to better quantify improvement from radiation therapy, the GBM model was used to predict what the tumor size (T2 MRI visible radius) would be for patient 1 and patient 2 over time if no radiation therapy was used. Quantitative results of tumor control are reported in terms of 'Treatment Gain' which is the difference of the time it takes for this baseline to reach a 4 cm T2 MRI visible radius versus the time it would take using various forms of radiation treatment as calculated by the model. Normal tissue EUD is used to quantify risk to normal tissue for these simplified example patients.

2.3. MOEA for IMRT optimization

A MOEA was used for IMRT optimization (Holdsworth *et al* 2010, Holdsworth *et al* 2011, Holdsworth *et al* 2012). The MOEA itself consists of two interacting algorithms each with its own set of objectives: (1) a deterministic IMRT optimization algorithm that generates IMRT plans by minimizing a penalty function that is a weighted sum of clinical objectives and (2) an evolutionary algorithm that selects superior (non-dominated) plans based on a separate set of decision criteria. The population of superior plans is used to generate new formulations of the penalty function which can be minimized to produce new IMRT plans. Using this process of natural selection, the MOEA will produce sets of IMRT plans that approach the Pareto Front and represent the best possible tradeoff amongst decision criteria.

Deterministic multiobjective IMRT algorithms minimize fitness criteria, and then use those same criteria to judge plan quality in the selection process; however, this requires that all fitness criteria are of a mathematical form that lends itself to efficient optimization. The MOEA is a stochastic multiobjective algorithm that uses a set of penalty objectives for individual IMRT optimization, and uses a separate set of decision criteria to judge plan quality in the selection process of the evolutionary algorithm. While the penalty objectives in our algorithm are quadratic, the decision criteria have no mathematical restrictions and can be designed solely to emulate to most appropriate clinical goals. Another advantage is that the set of decision criteria can be kept small for more efficient multiobjective optimization (Holdsworth *et al*

2011), while the set of penalty objectives can be expanded for greater flexibility in the search for more optimal IMRT plans (Holdsworth *et al* 2012).

The IMRT optimization utilized in our MOEA minimizes a fairly standard penalty function that is a weighted sum of quadratic penalty objectives:

$$\sum\sum H_i(D_{\text{ref},i} - d_{i,j})\, W_i(D_{\text{ref},i} - d_{i,j})^2 + F_s \tag{5}$$

where $d_{i,j}$ is dose in the jth voxel of the ith structure, W_i is the weight of the ith structure, $D_{\text{ref},i}$ is the reference dose parameter that defines the ith structure's penalty objective, F_s is a smoothing matrix that ensures the fluence can be translated into a deliverable beam, and $H_i(D_{\text{ref},i} - d_{i,j})$ is a Heaviside function that sets the weight to 0 in OAR voxels when $D_{\text{ref},i} > d_{i,j}$ and is 1 otherwise. Each iteration, the evolutionary algorithm generates sets of W_i and D_{ref}, based on recombination and mutation from existing non-dominated plans that formulate a new penalty function. This penalty function is minimized generating a new IMRT plan. For this work, the quality of the plan is judged by three decision criteria described below, and all plans are compared and any dominated plans are eliminated prior to beginning the next iteration of the MOEA.

This stochastic algorithm has the advantages of being able to incorporate any form of decision criteria and of not requiring *a priori* determination of the importance of each criterion. The algorithm returns Pareto optimal plans with respect to the decision criteria utilized in the multiobjective optimization. In this work, three decision criteria were used. Two criteria were used to evaluate all plans: (1) minimizing the maximum dose per fraction to any voxel and (2) minimizing normal tissue EUD. The third decision criterion was varied in order to see the effects of altering target optimization objectives: (3a) tumor cell kill, (3b) tumor survival after 1 week of treatment or (3c) tumor survival 11 weeks after 1 week of treatment. For criteria (3b) and (3c), the GBM model was used to predict tumor growth from that stage of the optimization process. These criteria were used in the weekly adaptive optimization process. Each fraction was scaled such that the EUD to normal brain was less than or equal to that of the standard-of-care plan and such that the maximum dose per fraction to any voxel in the scaled dose distribution was also limited by a given maximum dose (3 Gy, 8 Gy, or no limit).

In this work, the optimal distribution for each week of treatment is generated in 300 iterations, and 7 weeks of treatment are generated for each scenario. Optimization of all of the distributions throughout the 34 fractions to be delivered to one patient takes anywhere from 6 min to 10 h. When maximum cell kill is used as target decision criteria and there is a low allowed maximum dose, the adaptive optimization is much faster. If decision criteria for the target is calculated using the model to simulate 12 weeks of response for each iteration and if no maximum dose is used, the optimization takes much longer. The optimal distribution to be used in the GBM model for each week of treatment is selected based on a weighted sum of decision criteria. The GBM model then simulates of growth, diffusion and radiation damage for five days using this radiation dose distribution and two weekend days without radiation. The resulting tumor cell distribution is used for the following week's optimization.

For ease of model integration and computation, simulations were carried out in a simplified three-dimensional geometry where the tumor cell density was spherically symmetric and the structures in the optimization consisted of concentric shells. Each shell had its own proportion of tumor cells and genes (objectives and weights used in the penalty function) to be optimized by the MOEA. In this work, the simulations included a few sets of simple decision criteria, but other objectives such as dose to specific structures, DVH information or any quantifiable metrics specific to a given clinical situation can be used to either judge or scale dose distributions.

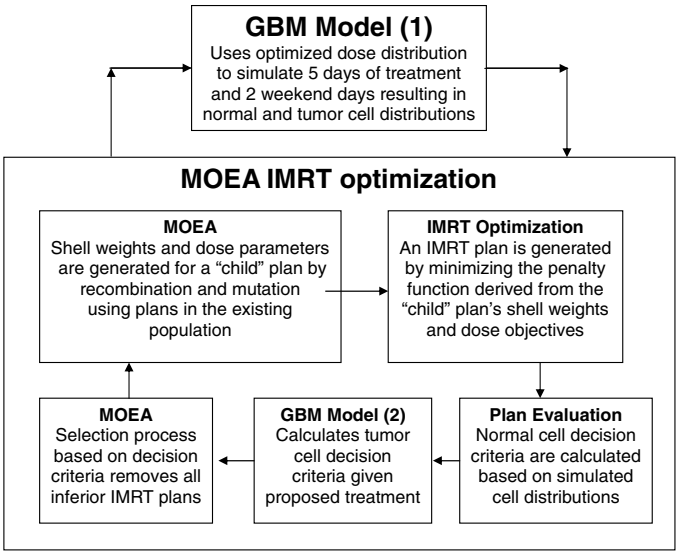

Figure 1. A diagram of the data flow between the GBM model and the MOEA IMRT optimization algorithm. The GBM model is used to (1) simulate each week of treatment *and* (2) calculate decision criteria in the MOEA.

Adaptive therapy was implemented by performing weekly MOEA IMRT optimizations using the most up-to-date predictions of tumor cell distributions obtained from the GBM model. Each week of treatment is simulated with the GBM model using the generated dose distribution to determine the tumor cell density used in the next round of optimization. Figure 1 demonstrates the iterative dialogue between the two algorithms.

The results of the optimizations were compared using four metrics:

(1) tumor radius as would be visible on T2 MRI;
(2) dose–volume histograms of total normal tissue EUD outside of the T2 enhancing region;
(3) dose–volume histograms of total tumor tissue EUD;
(4) treatment gain, the delay in days for the T2 radius to reach 4 cm compared to the untreated control.

3. Results

3. 1. Tumor control performance

In each simulation, three decision criteria were used to judge plan quality. Two of these criteria are used in every simulation while the third criterion was varied to test different models of tumor control. Results are reported in terms of the T2 MRI radius over time as predicted by the GBM model, treatment gain, and normal tissue EUD.

The predicted radius of the T2 MRI region over time is plotted for the standard plan and for the results of five different MOEA optimizations in figure 2. Three of the optimized plans were generated using minimum tumor cell survival after 1 week of treatment as the tumor control decision criteria with three different maximum dose/fraction restrictions: 3 Gy, 8 Gy, and no restriction. The other two MOEA optimizations shown use an 8 Gy/fraction maximum

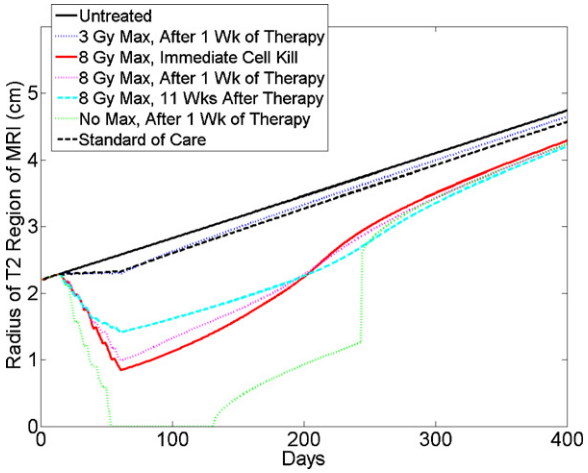

Figure 2. Plot of simulated T2 MRI radii versus time for the first patient. The untreated case and the standard protocol are compared to MOEA optimized dose distributions using maximum allowed doses per fraction of 3 Gy, 8 Gy and no maximum (all using one week tumor survival decision criteria). Also included are simulations using tumor cell kill and tumor survival 12 weeks after treatment (both using an 8 Gy maximum dose restriction).

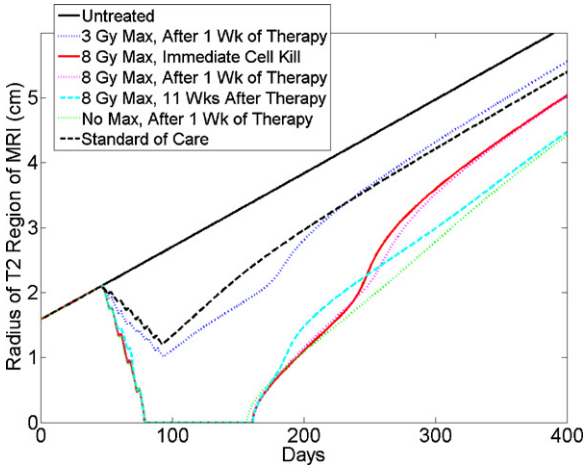

Figure 3. Plot of simulated T2 MRI radii versus time for the second patient. The untreated case and standard protocol are compared to optimized dose distributions using maximum allowed doses per fraction of 3 Gy, 8 Gy and no maximum (all using 1 week tumor survival decision criteria). Also included are simulations using tumor cell kill and tumor survival 12 weeks after treatment (both using an 8 Gy maximum dose restriction).

dose restriction using either maximum tumor cell kill per fraction or minimum tumor survival 12 weeks later for tumor control decision criteria. Similar results are shown in figure 3 for the second example patient.

A summary of results are in table 2 below. Normal tissue EUD is calculated by solving equation (1) iteratively. Treatment gain is the added number of days for the T2 MRI radii to reach 4 cm using RT versus no treatment.

Table 2.

Radiation therapy plan	Normal tissue EUD (Gy)	Treatment gain (days)
Patient 1		
Standard	1.00	27
3 Gy maximum with tumor survival after 1 week	0.22	16
8 Gy maximum with tumor survival after 1 week	0.81	84
No maximum with tumor survival after 1 week	0.85	84
8 Gy maximum with tumor cell kill	0.71	77
8 Gy maximum with tumor survival after 12 weeks	0.82	90
Patient 2		
Standard	1.00	68
3 Gy maximum with tumor survival after 1 week	0.27	61
8 Gy maximum with tumor survival after 1 week	0.56	113
No maximum with tumor survival after 1 week	0.93	157
8 Gy maximum with tumor cell kill	0.55	111
8 Gy maximum with tumor survival after 12 weeks	0.87	153

Note that for some simulations, the radius plot shows a steep jump in radius before resuming linear growth. This does not represent change in overall growth rate, but instead occurs when a large region of the tumor cell population achieves the minimum T2 cell density still visible on an MRI image. This reflects the complex interplay between a diffuse distribution of gliomas cells and the ability to reach a local threshold of detection to be visible on MRI.

For both patients, optimized plans with the maximum dose per fraction limited to 3 Gy resulted in response slightly worse than the standard plan for one-fourth the dose to normal tissue. For patient 1 that had lower parameter values for the net proliferation rate, ρ, and radiosensitivity, the treatment gain was lower for all RT plans, and results were similar for all optimized plans with maximum dose per fraction $>$ 3 Gy. For patient 2 that had larger values for the net proliferation rate, ρ and radiosensitivity, tumor response was highly dependent on both the maximum dose and the tumor control decision criterion implemented. When no maximum dose was used, the treatment gain improved to 157 days; however, the high dose in small volumes of tissue would be prohibitive for practical use in the clinical. The MOEA optimized treatment scheme that used tumor survival 12 weeks post treatment demonstrated the best simulated performance for this patient with a treatment gain of 153 days. All results were simulated by the GBM model for two simplified example patients.

3.2. Tumor cell population dose volume histograms

Cumulative dose volume histograms (DVHs) are used to demonstrate how different tumor decision criteria and maximum dose restrictions affect dose distributions. In figure 4, DVHs using total dose delivered in 34 fractions to the tumor cell population for the standard plan compared to the five same MOEA optimized dose distributions as in figures 2 and 3 for the second patient are displayed.

The maximum dose restriction directly affects the dose delivered to the bulk of the tumor; however, the predicted tumor control of the plan that used 11 weeks after 1 week of treatment cell survival as decision criteria had a much lower dose level and performance that was comparable to the MOEA plan that did not have a maximum dose restriction according to the GBM model. This result implies that the location of tumor cells targeted for radiation therapy

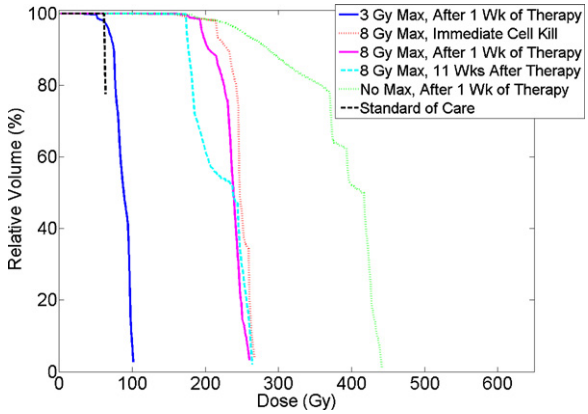

Figure 4. Dose volume histograms of the tumor cell population are displayed for the standard plan and for the MOEA optimized plans using 1 week tumor survival decision criteria with either a 3 Gy restriction on maximum dose, an 8 Gy restriction on maximum dose or without restriction. Also shown are DVHs for the MOEA plans that used 8 Gy maximum dose and either tumor cell kill or tumor population 11 weeks after 1 week of treatment.

is as important as dose level to the tumor core when it comes to predicted long term tumor control. There is wide patient-to-patient variation in the extent of diffusely invaded tumor cells peripheral to the imaging abnormality (Harpold *et al* 2007, Wang *et al* 2009a, Szeto *et al* 2009, Rockne *et al* 2010) that supports the need for patient-individualized treatment optimization to carefully incorporate this diffuse disease extent.

Without setting a maximum dose, the optimization can reach doses over small volumes that are far higher than current clinical practice. By forcing the maximum dose of optimizations to be lower, distributions will be more acceptable for clinical use, but tumor control may be sacrificed. As previously discussed (Holdsworth *et al* 2011), the specific goals or decision criteria used during multiobjective optimization play an important role in the final dose distributions and the quality of the radiation therapy with regard to what is best for the patient.

3.3. Normal tissue dose volume histograms

In figure 5, DVHs of the normal cell population for the optimized dose distributions for the second patient are compared to the DVHs resulting from the conventional clinical radiation therapy. Minimum tumor cell survival after 1 week of treatment is used as decision criteria in the MOEA for three optimizations using different restrictions on maximum dose. DVHs for normal tissue are also displayed for two other MOEA optimizations using maximum tumor cell kill and minimum tumor cell survival 12 weeks after radiation therapy that are also displayed (both with an 8 Gy maximum dose restriction).

4. Discussion

In this work, we report on a novel integration of an IMRT optimization algorithm with a spatially and temporally dependent glioma tumor response model. This integration has allowed for potential adaptation of the radiation delivery in response to changes in the tumor due to radiation killing, diffusion and proliferation of the tumor cells. The use of a multiobjective

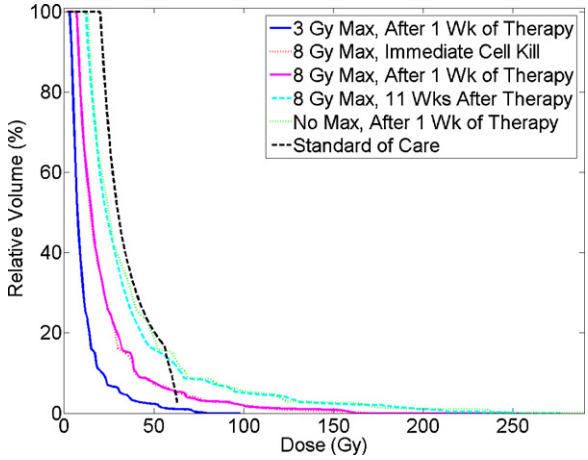

Figure 5. Dose volume histograms of the normal brain cell population are displayed for the standard plan and MOEA optimized plans using 1 week predicted tumor survival decision criteria with either a 3 Gy restriction per fraction on maximum dose, an 8 Gy per fraction restriction on maximum dose or without a maximum dose per fraction restriction for the second patient. Normal tissue DVHs are also shown for two optimizations using an 8 Gy restriction with either tumor cell kill or tumor survival 12 weeks after treatment.

optimization algorithm provides a means of searching for the best set of IMRT plans without needing to make decisions regarding the relative importance of the clinical goals before it is known what can be achieved. The choice of a stochastic MOEA has allowed us to use a number of different objectives (mathematical forms of clinical goals) that are difficult to use in deterministic optimization algorithms. These *decision criteria* provide a robust method for searching and evaluating different IMRT plans.

The use of a space-, time- and radiation-dependent model of tumor growth and distribution highlights the role that high-level biological models can play in radiation therapy. The fact that this particular model uses measured patient-specific parameters is a significant step beyond the normal use of radiobiological models in treatment optimization. In addition, the model allows us to investigate two aspects of adaptive therapy that have not been explored to any great extent, namely, to adapt the dose distribution to changes in physical distribution of the tumor and to adapt to the temporal evolution of the system.

With respect to the spatial distribution, results predicted by the mathematical model for two simplified patient examples suggest that the standard plan of uniform dose to the bulk of the tumor with a 2.5 cm margin has the potential to be improved in terms of both tumor control and normal tissue dose. MOEA optimized doses that used biological decision criteria based on a mathematical model of GBM and were adapted as the predicted tumor cell distribution changed for each week of treatment demonstrated the potential for improvement in tumor control and lower normal tissue EUD over current standard clinical practice. In results predicted by the GBM model, restricting the maximum dose per fraction to 3 Gy diminished the performance of optimized plans to control tumor invasion to the level of the standard plan; however, the EUD delivered to normal tissue in the brain was reduced by about a factor of 4 for the two simplified patient examples. Due to the greater normal tissue sparing, one outcome could be designing dose/fractionation schedules that increase the total amount of radiation while keeping the potential risks low.

When the maximum dose restriction was increased to 8 Gy per fraction, simulated tumor control was greatly enhanced. When no restriction was used, tumor control performance improved further; however, the MOEA plan that used predicted tumor cell survival 11 weeks post treatment for tumor control decision criteria and an 8 Gy maximum dose also demonstrated the same performance for the patient. This suggests that targeting certain glioblastoma cells in locations on or just outside the edge of the tumor could be as effective as delivering high doses with high risk of brain tissue necrosis to the bulk of the tumor. One of the difficulties of this study has been in modeling the effect on normal tissue when the insidious nature of GBM results in a mixture between brain and tumor.

With respect to advantages of adapting the IMRT delivery to the temporal development of the tumor, figures 2 and 3 and table 2 show the potential advantage of using the model to predict future growth and optimizing the dose based on that prediction. We have accounted for time-dependent tumor response by performing adaptive planning during the course of delivery and by designing decision criteria that evaluate the future state of the tumor. A more general approach that uses a stochastic model of tumor response has been described by Kim *et al* (2009, 2012) in which a Markov Decision Process is developed assuming periodic studies (imaging) that provide information regarding tumor response. This model also results in optimal treatment plans that vary the dose per fraction, as well as the spatial dose distribution, according to the development of the tumor. Other approaches to account for stochastic radiation effects have usually relied on applying probability distribution functions of parameters (Webb and Nahum 1993).

The optimized MOEA treatment schemes deliver higher doses to smaller volumes of tissue such that each fraction delivers an EUD to normal tissue outside of the T1Gd enhancement that is less than or equal to that of the standard plan. The MOEA is flexible and will optimize on whatever decision criteria it is given. If the 'high dose tails' in the optimized plans are clinically unacceptable, a different set of decision criteria could be employed to minimize them. Mathematically, the large volumes of lower dose compensate for the small volumes of high dose in the normal tissue EUD formula.

When large margins are added to targeted volumes in radiation therapy to account for set up error, the PTV volumes are greatly increased. This results in much higher dose to large volumes of normal tissue relative to that of the tumor cell population. Precise, non-uniform dose distributions in radiation therapy would have to be used in conjunction with accurate localization and immobilization to minimize set up margins and take advantage of the benefits of non-uniform, biologically optimized dose distributions.

5. Conclusions

Using data from two simple example patients, a patient-specific mathematical model of glioblastoma demonstrated how adaptive radiation therapy using biological optimization of tumor cell control and normal tissue sparing has the potential to improve patient outcome. These results also suggest that using clinical objectives and decision criteria that focus on future states of the tumor has the potential to generate more efficacious dose distributions. A powerful aspect of this combined technique is the flexibility of the MOEA to adapt to any input data and to optimize to any desired end point while being informed by a patient-specific understanding of the proliferation and invasion kinetics of cancerous cells. The long term potential of this approach is greater as modeling becomes more detailed, as more effective decision criteria tailored to specific clinical situations are employed, and by utilizing voxel-specific IMRT objectives (Holdsworth *et al* 2012) so that any patient can be optimized regardless of complexity. This work demonstrates the roles that a robust model of tumor growth and radiation

response and increased information from imaging could play in improving radiation therapy for tumors that are difficult to treat, such as glioblastoma. The multiobjective optimization platform provided a powerful and flexible method for implementing these models in a clinically useful fashion that provides the decision maker with a range of achievable choices.

Acknowledgments

We gratefully acknowledge NIH grants RO1CA112505 and R01NS060752 as well as the support of the James S McDonnell Foundation.

References

Binda E, Visioli A, Reynolds B and Vescovi A L 2012 Heterogeneity of cancer-Initiating cells within glioblastoma *Front. Biosci. (Schol Ed)* **4** 1235–48

Brown J M 2000 Exploiting the hypoxic cancer cell: mechanisms and therapeutic strategies *Mol. Med. Today* **6** 157–62

Carlson D J, Keall P J, Loo B W, Chen Z J and Brown J M 2011 Hypofractionation results in reduced tumor cell kill compared to conventional fractionation for tumors with regions of hypoxia *Int. J. Radiat. Oncol. Biol. Phys.* **79** 1188–95

Fisher R A 1937 The wave of advance of advantageous genes *Ann. Eugenics* **7** 353–69

Hall E 1994 Radiobiology for the Radiologist (Philadelphia: J.B. Lippincott Company)

Harpold H L P, Alvord E C and Swanson K R 2007 The evolution of mathematical modeling of glioma growth and invasion *J. Neuropathol. Exp. Neurol.* **66** 1–9

Holdsworth C H, Kim M, Liao J and Phillips M H 2010 A hierarchical evolutionary algorithm for multiobjective optimization in IMRT *Med. Phys.* **37** 4986–97

Holdsworth C H, Kim M, Liao J and Phillips M H 2011 Investigation of effective decision criteria for multiobjective optimization in IMRT *Med. Phys.* **38** 2964–74

Holdsworth C H, Kim M, Liao J and Phillips M H 2012 The use of a multiobjective evolutionary algorithm to increase flexibility in the search for better IMRT plans *Med. Phys.* **39** 2261–74

Kim M, Ghate A and Phillips M 2009 A Markov decision process approach to temporal modulation of dose fractions in radiation therapy planning *Phys. Med. Biol.* **54** 4455–76

Kim H, Ghate A and Phillips M 2012 A stochastic control formalism for dynamic biologically conformal radiation therapy *Eur. J. Operational Research* **219** (3) 541–56

Lawrence Y R, Li X A, el Naqa I, Hahn C A, Marks L B, Merchant T E and Dicker A P 2010 Radiation dose-volume effects in the brain *Int. J. Radiat. Oncol. Biol. Phys.* **76** 20–7

Mandonnet E, Delattre H Y, Tanguy M L, Swanson K R, Carpentier A F, Duffau H, Cornu P, Van Effenterre R, Alvord E C and Capelle L 2003 Continuous growth of mean tumor diameter in a subset of WHO grade II gliomas *Ann. Neurol.* **53** 524–8

Niemierko A 1997 Reporting and analyzing dose distributions: a concept of equivalent uniform dose *Med. Phys.* **24** 103–10

Perez-Garcia A, Carrion-Navarro J, Bosch-Fortea M, Lazaro-Ibanez E, Prat-Acin R and Ayuso-Sacido A 2012 Genomic instability of surgical sample and cancer-initiating cell lines from human glioblastoma *Front. Biosci.* **17** 1469–79

Rockne R, Alvord E C, Rockhill J K and Swanson K R 2009a A mathematical model for brain tumor response to radiation therapy *J. Math. Biol.* **58** 561–78

Rockne R, Alvord E C and Swanson K R 2009b Prognostic significance of growth kinetics in newly diagnosed glioblastomas revealed by combining serial imaging with a novel biomathematical model *Cancer Res.* **69** 9133–40

Rockne R, Rockhill J K, Mrugala M, Spence A M, Kalet I, Hendrickson K, Lai A, Cloughesy T, Alvord E C and Swanson K R 2010 Predicting the efficacy of radiotherapy in individual glioblastoma patients in vivo: a mathematical modeling approach *Phys. Med. Biol.* **55** 3271–85

Sachs R K, Hahnfeld P and Brenner D J 1997 The link between low-LET dose-response relations and the underlying kinetics of damage production/repair/misrepair *Int. J. Radiat. Biol.* **72** 351–74

Stewart R D and Li X A 2007 BGRT: biologically guided radiation therapy—the future is fast approaching! *Med. Phys.* **34** 3739–51

Stupp R *et al* 2005 Radiotherapy plus concomitant and adjuvant temozolomide for glioblastoma *N. Engl. J. Med.* **352** 987–96

Swanson K R, Bridge C, Murray J D and Alvord E C 2003 Virtual and real brain tumors: using mathematical modeling to quantify glioma growth and invasion *J. Neurol. Sci.* **216** 1–10

Swanson K R, Harpold H L P, Peacock D L, Rockne R, Pennington C, Kilbride L, Grant R, Wardlaw J and Alvord E C 2008a Velocity of radial expansion of contrast-enhancing gliomas and effectiveness of radiotherapy in individual patients: a proof of principle *Clin. Oncol.* **20** 301–8

Swanson K R, Rostomily R and Alvord E C 2008b Predicting survival of patients with glioblastoma by combining a mathematical model and pre-operative MR imaging characteristics: a proof of principle *Br. J. Cancer* **98** 113–9

Swanson K R and Alvord E C Jr 2002 Serial imaging observations and postmortem examination of an untreated glioblastoma: a traveling wave of glioma growth and invasion *Neuro-Oncol.* 4340

Szeto M D, Chakraborty G, Hadley J, Rockne R, Muzi M, Alvord E C Jr, Krohn K A, Spence A M and Swanson K R 2009 Quantitative metrics of net proliferation and invasion link biological aggressiveness assessed by MRI with hypoxia assessed by FMISO-PET in newly diagnosed glioblastomas *Cancer Res.* **69** 4502–9

Tome W A and Fowler J F 2003 On the inclusion of proliferation in tumour control probability calculations for inhomogeneously irradiated tumours *Phys. Med. Biol.* **48** 261–8

Wang C H *et al* 2009a Prognostic significance of growth kinetics in newly diagnosed glioblastomas revealed by combining serial imaging with a novel biomathematical model *Cancer Res.* **69** 9133–40

Wang C H *et al* 2009b Quantitative metrics of net proliferation and invasion link biological aggressiveness assessed by MRI with hypoxia assessed by FMISO-PET in newly diagnosed glioblastomas *Cancer Res.* **69** 4502–9

Webb S and Nahum A E 1993 A model for calculating tumour control probability in radiotherapy including the effects of inhomogeneous distributions of dose and clonogenic cell density *Phys. Med. Biol* **38** 653–66